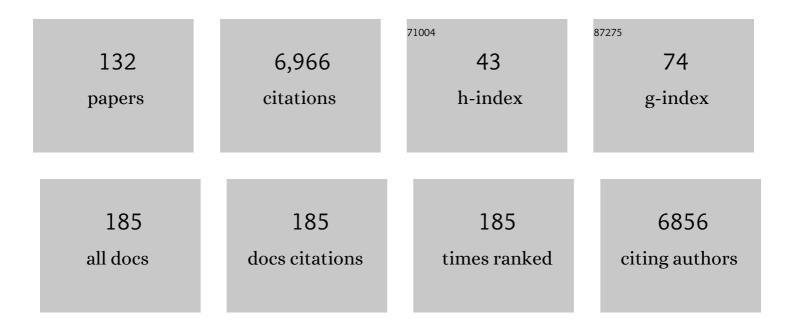
List of Publications by Year in descending order

Source: https://exaly.com/author-pdf/5544804/publications.pdf Version: 2024-02-01



#	Article	IF	CITATIONS
1	Black carbon aerosols over the Himalayas: direct and surface albedo forcing. Tellus, Series B: Chemical and Physical Meteorology, 2022, 65, 19738.	0.8	118
2	The SALTENA Experiment: Comprehensive Observations of Aerosol Sources, Formation, and Processes in the South American Andes. Bulletin of the American Meteorological Society, 2022, 103, E212-E229.	1.7	9
3	Particulate Matter Ionic and Elemental Composition during the Winter Season: A Comparative Study among Rural, Urban and Remote Sites in Southern Italy. Atmosphere, 2022, 13, 356.	1.0	4
4	Development and evolution of an anomalous Asian dust event across Europe in March 2020. Atmospheric Chemistry and Physics, 2022, 22, 4047-4073.	1.9	8
5	Enhanced confinement in diverted negative-triangularity L-mode plasmas in TCV. Plasma Physics and Controlled Fusion, 2022, 64, 014004.	0.9	15
6	On the Redox-Activity and Health-Effects of Atmospheric Primary and Secondary Aerosol: Phenomenology. Atmosphere, 2022, 13, 704.	1.0	7
7	Biogenic particles formed in the Himalaya as an important source of free tropospheric aerosols. Nature Geoscience, 2021, 14, 4-9.	5.4	40
8	Changes in black carbon emissions over Europe due to COVID-19 lockdowns. Atmospheric Chemistry and Physics, 2021, 21, 2675-2692.	1.9	40
9	Intercomparison and characterization of 23 Aethalometers under laboratory and ambient air conditions: procedures and unit-to-unit variabilities. Atmospheric Measurement Techniques, 2021, 14, 3195-3216.	1.2	22
10	Examination of stiff ion temperature gradient mode physics in simulations of DIII-D H-mode transport. Nuclear Fusion, 2021, 61, 066033.	1.6	12
11	Diverted negative triangularity plasmas on DIII-D: the benefit of high confinement without the liability of an edge pedestal. Nuclear Fusion, 2021, 61, 116010.	1.6	20
12	Ballooning instability preventing the H-mode access in plasmas with negative triangularity shape on the DIII–D tokamak. Plasma Physics and Controlled Fusion, 2021, 63, 105006.	0.9	25
13	Emerging Investigator Series: COVID-19 lockdown effects on aerosol particle size distributions in northern Italy. Environmental Science Atmospheres, 2021, 1, 214-227.	0.9	12
14	Comparison of co-located refractory black carbon (rBC) and elemental carbon (EC) mass concentration measurements during field campaigns at several European sites. Atmospheric Measurement Techniques, 2021, 14, 1379-1403.	1.2	19
15	A brief history of negative triangularity tokamak plasmas. Reviews of Modern Plasma Physics, 2021, 5, 1.	2.2	21
16	The role of toroidal rotation in the very high energy confinement quality observed in super H-mode experiments on DIII-D. Physics of Plasmas, 2021, 28, .	0.7	4
17	Seasonality of the particle number concentration and size distribution: a global analysis retrieved from the network of Global Atmosphere Watch (GAW) near-surface observatories. Atmospheric Chemistry and Physics, 2021, 21, 17185-17223.	1.9	31
18	Increasing the maturity of measurements of essential climate variables (ECVs) at Italian atmospheric WMO/GAW observatories by implementing automated data elaboration chains. Computers and Geosciences, 2020, 137, 104432.	2.0	5

#	Article	IF	CITATIONS
19	Long-term observations of aerosol optical properties at three GAW regional sites in the Central Mediterranean. Atmospheric Research, 2020, 241, 104976.	1.8	10
20	Advection pathways at the Mt. Cimone WMO-GAW station: Seasonality, trends, and influence on atmospheric composition. Atmospheric Environment, 2020, 234, 117513.	1.9	11
21	Spatial and Temporal Variability of Carbonaceous Aerosol Absorption in the Po Valley. Aerosol and Air Quality Research, 2020, 20, 2624-2639.	0.9	12
22	Multidecadal trend analysis of in situ aerosol radiative properties around the world. Atmospheric Chemistry and Physics, 2020, 20, 8867-8908.	1.9	58
23	Cézeaux-Aulnat-Opme-Puy De Dôme: a multi-site for the long-term survey of the tropospheric composition and climate change. Atmospheric Measurement Techniques, 2020, 13, 3413-3445.	1.2	26
24	A global analysis of climate-relevant aerosol properties retrieved from the network of Global Atmosphere Watch (GAW) near-surface observatories. Atmospheric Measurement Techniques, 2020, 13, 4353-4392.	1.2	65
25	Investigation of potential source regions of atmospheric Black Carbon in the data deficit region of the western Himalayas and its foothills. Atmospheric Pollution Research, 2019, 10, 1832-1842.	1.8	18
26	New Particle Formation: A Review of Ground-Based Observations at Mountain Research Stations. Atmosphere, 2019, 10, 493.	1.0	26
27	Alfvén eigenmodes and fast ion transport in negative triangularity DIII-D plasmas. Nuclear Fusion, 2019, 59, 086028.	1.6	17
28	H-mode grade confinement in L-mode edge plasmas at negative triangularity on DIII-D. Physics of Plasmas, 2019, 26, .	0.7	38
29	Achievement of Reactor-Relevant Performance in Negative Triangularity Shape in the DIII-D Tokamak. Physical Review Letters, 2019, 122, 115001.	2.9	86
30	A combined Phase Contrast Imaging and heterodyne interferometer for multiscale fluctuation measurements in tokamak plasmas. Journal of Instrumentation, 2019, 14, C12023-C12023.	0.5	2
31	Ground level ice nucleating particles measurements at Capo Granitola, a Mediterranean coastal site. Atmospheric Research, 2019, 219, 57-64.	1.8	6
32	Indoor air pollution exposure effects on lung and cardiovascular health in the High Himalayas, Nepal: An observational study. European Journal of Internal Medicine, 2019, 61, 81-87.	1.0	26
33	Multi-scale transport in the DIII-D ITER baseline scenario with direct electron heating and projection to ITER. Physics of Plasmas, 2018, 25, .	0.7	18
34	Seasonal variability of carbonaceous aerosols in an urban background area in Southern Italy. Atmospheric Research, 2018, 200, 97-108.	1.8	39
35	Seasonal variability of PM2.5 and PM10 composition and sources in an urban background site in Southern Italy. Science of the Total Environment, 2018, 612, 202-213.	3.9	136
36	Experimental challenges to stiffness as a transport paradigm. Nuclear Fusion, 2018, 58, 026023.	1.6	11

#	Article	IF	CITATIONS
37	Characterization of In Situ Aerosol Optical Properties at Three Observatories in the Central Mediterranean. Atmosphere, 2018, 9, 369.	1.0	19
38	Vertical distribution of aerosol optical properties in the Po Valley during the 2012 summer campaigns. Atmospheric Chemistry and Physics, 2018, 18, 5371-5389.	1.9	11
39	AÂEuropean aerosol phenomenology – 6: scattering properties of atmospheric aerosol particles from 28ÂACTRIS sites. Atmospheric Chemistry and Physics, 2018, 18, 7877-7911.	1.9	76
40	New "Smart―Systems for Atmospheric Aerosol and Reactive Gas Sampling in Ambient Air. Sensors, 2018, 18, 3602.	2.1	1
41	A combined phase contrast imaging and heterodyne interferometer system for multiscale fluctuation measurements (invited). Review of Scientific Instruments, 2018, 89, 10B106.	0.6	6
42	Identification of topographic features influencing aerosol observations at high altitude stations. Atmospheric Chemistry and Physics, 2018, 18, 12289-12313.	1.9	31
43	Fractal-like Tar Ball Aggregates from Wildfire Smoke. Environmental Science and Technology Letters, 2018, 5, 360-365.	3.9	29
44	Black Carbon and Ozone Variability at the Kathmandu Valley and at the Southern Himalayas: A Comparison between a "Hot Spot―and a Downwind High-Altitude Site. Aerosol and Air Quality Research, 2018, 18, 623-635.	0.9	16
45	Magnetic shear effects on plasma transport and turbulence at high electron to ion temperature ratio in DIII-D and JT-60U plasmas. Nuclear Fusion, 2017, 57, 056027.	1.6	10
46	Atmospheric Ice Nucleating Particle measurements at the high mountain observatory Mt. Cimone (2165Âm a.s.l., Italy). Atmospheric Environment, 2017, 171, 173-180.	1.9	11
47	The effect of electron cyclotron heating on density fluctuations at ion and electron scales in ITER baseline scenario discharges on the DIII-D tokamak. Nuclear Fusion, 2017, 57, 126014.	1.6	3
48	Inter-Comparison of Carbon Content in PM2.5 and PM10 Collected at Five Measurement Sites in Southern Italy. Atmosphere, 2017, 8, 243.	1.0	53
49	Investigation of reactive gases and methane variability in the coastal boundary layer of the central Mediterranean basin. Elementa, 2017, 5, .	1.1	17
50	Role of density gradient driven trapped electron mode turbulence in the H-mode inner core with electron heating. Physics of Plasmas, 2016, 23, 056112.	0.7	33
51	Intercomparison of 15 aerodynamic particle size spectrometers (APS 3321): uncertainties in particle sizing and number size distribution. Atmospheric Measurement Techniques, 2016, 9, 1545-1551.	1.2	39
52	A phase contrast imaging–interferometer system for detection of multiscale electron density fluctuations on DIII-D. Review of Scientific Instruments, 2016, 87, 11E117.	0.6	1
53	Summer atmospheric composition over the Mediterranean basin: Investigation on transport processes and pollutant export to the free troposphere by observations at the WMO/GAW Mt. Cimone global station (Italy, 2165Âm a.s.l.). Atmospheric Environment, 2016, 141, 139-152.	1.9	17
54	Multi-device studies of pedestal physics and confinement in the I-mode regime. Nuclear Fusion, 2016, 56, 086003.	1.6	54

#	Article	IF	CITATIONS
55	Light absorption properties of brown carbon in the high Himalayas. Journal of Geophysical Research D: Atmospheres, 2016, 121, 9621-9639.	1.2	83
56	Indoor pollution and respiratory health in the Himalayas. , 2016, , .		0
57	Seasonal variation of ozone and black carbon observed at Paknajol, an urban site in the Kathmandu Valley, Nepal. Atmospheric Chemistry and Physics, 2015, 15, 13957-13971.	1.9	56
58	Organic aerosol evolution and transport observed at Mt. Cimone (2165 m a.s.l.), Italy, during the PEGASOS campaign. Atmospheric Chemistry and Physics, 2015, 15, 11327-11340.	1.9	23
59	Black carbon in snow in the upper Himalayan Khumbu Valley, Nepal: observations and modeling of the impact on snow albedo, melting, and radiative forcing. Cryosphere, 2015, 9, 1685-1699.	1.5	57
60	Application of ECH to the Study of Transport in ITER Baseline Scenario-like Discharges in DIII-D. EPJ Web of Conferences, 2015, 87, 02003.	0.1	3
61	Characterization of density fluctuations during the search for an I-mode regime on the DIII-D tokamak. Nuclear Fusion, 2015, 55, 093019.	1.6	38
62	Investigating profile stiffness and critical gradients in shaped TCV discharges using local gyrokinetic simulations of turbulent transport. Plasma Physics and Controlled Fusion, 2015, 57, 054010.	0.9	35
63	Long-term surface ozone variability at Mt. Cimone WMO/GAW global station (2165 m a.s.l., Italy). Atmospheric Environment, 2015, 101, 23-33.	1.9	42
64	A 10 year record of black carbon and dust from a Mera Peak ice core (Nepal): variability and potential impact on melting of Himalayan glaciers. Cryosphere, 2014, 8, 1479-1496.	1.5	78
65	Transport of short-lived climate forcers/pollutants (SLCF/P) to the Himalayas during the South Asian summer monsoon onset. Environmental Research Letters, 2014, 9, 084005.	2.2	22
66	Influence of open vegetation fires on black carbon and ozone variability in the southern Himalayas (NCO-P, 5079ÂmÂa.s.l.). Environmental Pollution, 2014, 184, 597-604.	3.7	31
67	3-year chemical composition of free tropospheric PM1 at the Mt. Cimone GAW global station – South Europe – 2165Âm a.s.l Atmospheric Environment, 2014, 87, 218-227.	1.9	30
68	Spatial and seasonal variability of carbonaceous aerosol across Italy. Atmospheric Environment, 2014, 99, 587-598.	1.9	137
69	New atmospheric composition observations in the Karakorum region: Influence of local emissions and large-scale circulation during a summer field campaign. Atmospheric Environment, 2014, 97, 75-82.	1.9	8
70	Synoptic-scale dust transport events in the southern Himalaya. Aeolian Research, 2014, 13, 51-57.	1.1	10
71	In situ physical and chemical characterisation of the Eyjafjallajökull aerosol plume in the free troposphere over Italy. Atmospheric Chemistry and Physics, 2014, 14, 1075-1092.	1.9	12
72	Classification of clouds sampled at the puy de Dôme (France) based on 10 yr of monitoring of their physicochemical properties. Atmospheric Chemistry and Physics, 2014, 14, 1485-1506.	1.9	92

#	Article	IF	CITATIONS
73	Snow cover sensitivity to black carbon deposition in the Himalayas: from atmospheric and ice core measurements to regional climate simulations. Atmospheric Chemistry and Physics, 2014, 14, 4237-4249.	1.9	80
74	Variations in tropospheric submicron particle size distributions across the European continent 2008–2009. Atmospheric Chemistry and Physics, 2014, 14, 4327-4348.	1.9	41
75	Estimated range of black carbon dry deposition and the related snow albedo reduction over Himalayan glaciers during dry pre-monsoon periods. Atmospheric Environment, 2013, 78, 259-267.	1.9	70
76	Analysis of Summer Ozone Observations at a High Mountain Site in Central Italy (Campo Imperatore,) Tj ETQq0 0	0 rgBT /O	verlock 10 T
77	High black carbon and ozone concentrations during pollution transport in the Himalayas: Five years of continuous observations at NCO-P global GAW station. Journal of Environmental Sciences, 2013, 25, 1618-1625.	3.2	44
78	Validation studies of gyrofluid and gyrokinetic predictions of transport and turbulence stiffness using the DIII-D tokamak. Nuclear Fusion, 2013, 53, 083027.	1.6	22
79	Influence of biomass burning and anthropogenic emissions on ozone, carbon monoxide and black carbon at the Mt. Cimone GAW-WMO global station (Italy, 2165 m a.s.l.). Atmospheric Chemistry and Physics, 2013, 13, 15-30.	1.9	69
80	Mobility particle size spectrometers: harmonization of technical standards and data structure to facilitate high quality long-term observations of atmospheric particle number size distributions. Atmospheric Measurement Techniques, 2012, 5, 657-685.	1.2	689
81	Transport of Stratospheric Air Masses to the Nepal Climate Observatory–Pyramid (Himalaya; 5079 m) Tj ETQq1 1489-1507.	1 0.7843 0.6	14 rgBT /Ove 16
82	Only Coarse Particles From the Sahara?. Epidemiology, 2012, 23, 642-643.	1.2	9
83	Atmospheric Pollution in the Hindu Kush–Himalaya Region. Mountain Research and Development, 2012, 32, 468-479.	0.4	38
84	Hydrogen peroxide in natural cloud water: Sources and photoreactivity. Atmospheric Research, 2011, 101, 256-263.	1.8	40
85	Climatology of aerosol radiative properties in the free troposphere. Atmospheric Research, 2011, 102, 365-393.	1.8	121
86	Primary versus secondary contributions to particle number concentrations in the European boundary layer. Atmospheric Chemistry and Physics, 2011, 11, 12007-12036.	1.9	110
87	Number size distributions and seasonality of submicron particles in Europe 2008–2009. Atmospheric Chemistry and Physics, 2011, 11, 5505-5538.	1.9	214
88	Saharan dust and daily mortality in Emilia-Romagna (Italy). Occupational and Environmental Medicine, 2011, 68, 446-451.	1.3	99
89	Characterization and intercomparison of aerosol absorption photometers: result of two intercomparison workshops. Atmospheric Measurement Techniques, 2011, 4, 245-268.	1.2	284
90	Chemical composition of PM ₁₀ and PM ₁ at the high-altitude Himalayan station Nepal Climate Observatory-Pyramid (NCO-P) (5079 m a.s.l.). Atmospheric Chemistry and Physics, 2010, 10, 4583-4596.	1.9	141

#	Article	IF	CITATIONS
91	Seasonal variations of aerosol size distributions based on long-term measurements at the high altitude Himalayan site of Nepal Climate Observatory-Pyramid (5079 m), Nepal. Atmospheric Chemistry and Physics, 2010, 10, 10679-10690.	1.9	43
92	Sunphotometry of the 2006–2007 aerosol optical/radiative properties at the Himalayan Nepal Climate Observatory-Pyramid (5079 m a.s.l.). Atmospheric Chemistry and Physics, 2010, 10, 11209-11221.	1.9	41
93	Aerosol mass and black carbon concentrations, a two year record at NCO-P (5079 m, Southern) Tj ETQq1 1 0.7	′84314 rgE 1.9	BT /Overlock 1
94	Aerosol optical properties and radiative forcing in the high Himalaya based on measurements at the Nepal Climate Observatory-Pyramid site (5079 m a.s.l.). Atmospheric Chemistry and Physics, 2010, 10, 5859-5872.	1.9	87
95	Tropospheric ozone variations at the Nepal Climate Observatory-Pyramid (Himalayas, 5079 m a.s.l.) and influence of deep stratospheric intrusion events. Atmospheric Chemistry and Physics, 2010, 10, 6537-6549.	1.9	109
96	Atmospheric Brown Clouds in the Himalayas: first two years of continuous observations at the Nepal Climate Observatory-Pyramid (5079 m). Atmospheric Chemistry and Physics, 2010, 10, 7515-7531.	1.9	252
97	Estimated impact of black carbon deposition during pre-monsoon season from Nepal Climate Observatory – Pyramid data and snow albedo changes over Himalayan glaciers. Atmospheric Chemistry and Physics, 2010, 10, 6603-6615.	1.9	164
98	Characteristics of helmets, dissatisfaction with the helmet and accident risk: a case-control study. Injury Prevention, 2010, 16, A143-A143.	1.2	0
99	Road traffic accidents in the province of Milan (Italy): which risk factors?. Injury Prevention, 2010, 16, A119-A120.	1.2	2
100	Road accident causes among truck drivers: a multicentric study. Injury Prevention, 2010, 16, A143-A143.	1.2	0
101	Size-resolved aerosol chemical composition over the Italian Peninsula during typical summer and winter conditions. Atmospheric Environment, 2010, 44, 5269-5278.	1.9	99
102	Clarifications to the limitations of the s- $\hat{l}\pm$ equilibrium model for gyrokinetic computations of turbulence. Physics of Plasmas, 2009, 16, .	0.7	101
103	Angular Illumination and Truncation of Three Different Integrating Nephelometers: Implications for Empirical, Size-Based Corrections. Aerosol Science and Technology, 2009, 43, 581-586.	1.5	71
104	Stratospheric intrusion index (SI2) from baseline measurement data. Theoretical and Applied Climatology, 2009, 97, 317-325.	1.3	15
105	Influence of lower stratosphere/upper troposphere transport events on surface ozone at the Everest-Pyramid GAW Station (Nepal): first year of analysis. International Journal of Remote Sensing, 2009, 30, 4083-4097.	1.3	5
106	JET (³ He)–D scenarios relying on RF heating: survey of selected recent experiments. Plasma Physics and Controlled Fusion, 2009, 51, 044007.	0.9	47
107	The effect of plasma triangularity on turbulent transport: modeling TCV experiments by linear and non-linear gyrokinetic simulations. Plasma Physics and Controlled Fusion, 2009, 51, 055016.	0.9	61
108	Significant variations of trace gas composition and aerosol properties at Mt. Cimone during air mass transport from North Africa – contributions from wildfire emissions and mineral dust. Atmospheric Chemistry and Physics, 2009, 9, 4603-4619.	1.9	54

#	Article	IF	CITATIONS
109	Continuous measurements of aerosol physical parameters at the Mt. Cimone GAW Station (2165Âm asl,) Tj ETQ	q1 _{3.9} 0.78	4314 rgBT C
110	The ABC-Pyramid Atmospheric Research Observatory in Himalaya for aerosol, ozone and halocarbon measurements. Science of the Total Environment, 2008, 391, 252-261.	3.9	115
111	Effects of geometry on linear and non-linear gyrokinetic simulations, and development of a global version of the GENE code. , 2008, , .		1
112	High frequency new particle formation in the Himalayas. Proceedings of the National Academy of Sciences of the United States of America, 2008, 105, 15666-15671.	3.3	142
113	The physics of electron internal transport barriers in the TCV tokamak. Nuclear Fusion, 2007, 47, 714-720.	1.6	12
114	Critical temperature gradient length signatures in heat wave propagation across internal transport barriers in the Joint European Torus. Physics of Plasmas, 2007, 14, 092303.	0.7	8
115	10 The ABC-Pyramid: a scientific laboratory at 5079 m a.s.l. for the study of atmospheric composition change and climate. Developments in Earth Surface Processes, 2007, 10, 67-75.	2.8	1
116	Effect of selected organic and inorganic snow and cloud components on the photochemical generation of nitrite by nitrate irradiation. Chemosphere, 2007, 68, 2111-2117.	4.2	22
117	28 Chemical composition of fresh snow in the Himalaya and Karakoram. Developments in Earth Surface Processes, 2007, 10, 251-262.	2.8	2
118	Theoretical study of particle transport in electron internal transport barriers in TCV. AIP Conference Proceedings, 2006, , .	0.3	2
119	Speciation and role of iron in cloud droplets at the puy de Dôme station. Journal of Atmospheric Chemistry, 2006, 54, 267-281.	1.4	40
120	Analysis and modelling of power modulation experiments in JET plasmas with internal transport barriers. Plasma Physics and Controlled Fusion, 2006, 48, 1469-1487.	0.9	14
121	Probing Internal Transport Barriers with Heat Pulses in JET. Physical Review Letters, 2006, 96, 095002.	2.9	30
122	Design of a tangential phase contrast imaging diagnostic for the TCV tokamak. Review of Scientific Instruments, 2006, 77, 10E929.	0.6	27
123	Safety factor profile requirements for electron ITB formation in TCV. Plasma Physics and Controlled Fusion, 2005, 47, B107-B120.	0.9	22
124	Physicochemical properties of fine aerosols at Plan d'Aups during ESCOMPTE. Atmospheric Research, 2005, 74, 565-580.	1.8	9
125	Aerosol studies during the ESCOMPTE experiment: an overview. Atmospheric Research, 2005, 74, 547-563.	1.8	53
126	Cloud chemistry at the Puy de Dôme: variability and relationships with environmental factors. Atmospheric Chemistry and Physics, 2004, 4, 715-728.	1.9	121

#	Article	IF	CITATIONS
127	Transition Metal Ions in Cloud Chemistry. , 2004, , 569-579.		Ο
128	Contribution of gaseous and particulate species to droplet solute composition at the Puy de Dôme, France. Atmospheric Chemistry and Physics, 2003, 3, 1509-1522.	1.9	43
129	Chemical composition of freshsnow samples from the southern slope of Mt. Everest region (Khumbu-Himal region, Nepal). Atmospheric Environment, 2001, 35, 3183-3190.	1.9	53
130	Transmission of <i>Mycobacterium tuberculosis</i> to Contacts of HIV-infected Tuberculosis Patients. American Journal of Respiratory and Critical Care Medicine, 2001, 164, 2166-2171.	2.5	51
131	Mutations in Coagulation Factors in Women with Unexplained Late Fetal Loss. New England Journal of Medicine, 2000, 343, 1015-1018.	13.9	296
132	Long-term (2002–2012) investigation of Saharan dust transport events at Mt. Cimone GAW global station, Italy (2165 m a.s.l.). Elementa, 0, 4, 000085.	1,1	16